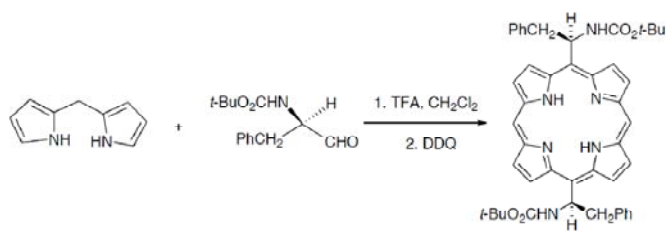Supporting Information

Water Redissoluble Chiral Porphyrin–Carbon Nanotube Composites

Xiaobin Peng,[*a] Hongmei Qin,[a] Lisheng Li,[a] Yuying Huang,[a] Junbiao Peng,[a] Yong Cao,[a] and Naoki Komatsu[b]

1. Synthesis of (R)- and (S)-5, 15-bis (1-*tert*-butoxycarbonylamino-2-phenylethyl) porphyrin ((R)- and (S)-**3**)

3

Chiral porphyrins ((R)- and (S)-**3** were synthesized starting from dipyrrylmethane and commercially available N-BOC-(R)- or -(S)-phenylalaninal. To a solution of 2,2'-dipyrrylmethane (292 mg, 2.0 mmol) and (R)-phenylalaninal (500 mg, 2.0 mmol) in CH_2Cl_2 (300 ml), trifluoroacetic acid (0.1 ml) was added and the mixture was stirred under Ar for 48 h at room temperature under dark. After the addition of DDQ (740 mg, 3.3 mmol), the mixture was stirred for additional 2 h. The reaction was quenched by the addition of triethylamine, and the reaction mixture was poured into water. The product was extracted with CH_2Cl_2 and purified by column chromatography using alumina and silica gel as stationary phases and CH_2Cl_2 as eluent. Further purification by recrystallization from $CHCl_3$ and acetonitrile gave 5,15-di(1'-*tert*-butoxycarbonylamino-2'-phenylethyl)porphyrin as purple solid in 19% yield (142 mg). (R)- and (S)-**3** gave the same ^{1}H NMR, absorption and mass spectra. HR-ESI-MS calcd for $C_{46}H_{49}N_6O_4$ ($M+H^+$): 749.38. Found: 749.38; UV-VIS ($CHCl_3$), λ_{max}: 406, 504, 537, 576 and 630 nm; ^{1}H NMR ($CDCl_3$, 270MHz), 10.20 (s, 2H), 9.57(4H, β-H), 9.38(4H, β-H), 7.37 (2H, phenyl), 6.80-7.00 (m, 8H, phenyl), 6.25(2H, C**H**CH$_2$Ph) 4.33(4H, CHC**H**$_2$Ph), 1.39 (s, 18H, *tert*-butyl), 0.85 (s, 2H, NH), -2.88(s, 2H, NH of pyrrole).

2. Synthesis of (R)- and (S)-5, 15-bis (1-amine-2-phenyl-ethyl) porphyrin ((R)- and (S)-**4**
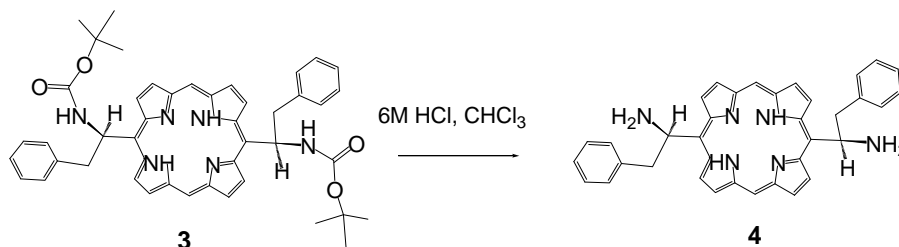
To a solution of **2** (112.2 mg, 0.15 mmol) in $CHCl_3$ (50 mL) was added 6M HCl (50mL) and stirred at room temperature until all porphyrin was extracted from organic layer to aqueous layer. After the separation of organic layer, the aqueous layer was neutralized with Na_2CO_3 solution, and then extracted with $CHCl_3$. The combined organic layer was washed with water, dried over Na_2SO_4, evaporated to dryness, and finally re-crystallized to give purple solid **4** (74.7 mg, yield: 91%) that was used for next reaction without further purification. (*R*)- and (*S*)-**4** gave the same ^{1}H NMR, absorption and mass spectra. UV-VIS($CHCl_3$): λ_{max}: 408, 505, 538, 578 and 633 nm. HR-ESI-MS calcd for $C_{36}H_{33}N_6$ (M+H^{+}) : 549.28. Found: 549.28. ^{1}H NMR ($CDCl_3$, 270MHz), 10.26 (s, 2H), 10.06 (br, 4H, β-H), 9.41(4H, β-H), 7.43 (4H, phenyl), 7.10-7.35 (m, 6H, phenyl), 6.93(2H, C*H*CH$_2$Ph) 4.15(4H, CHC*H*$_2$Ph), -2.88(s, 2H, NH of pyrrole).

3. Synthesis of (*R*)- and (*S*)-5,15-bis (1- (1',3'-isophthalic acid disodium salt-5'-carbamoyl)-2-phenyl-ethyl) porphyrin Zn (II) (**1**)
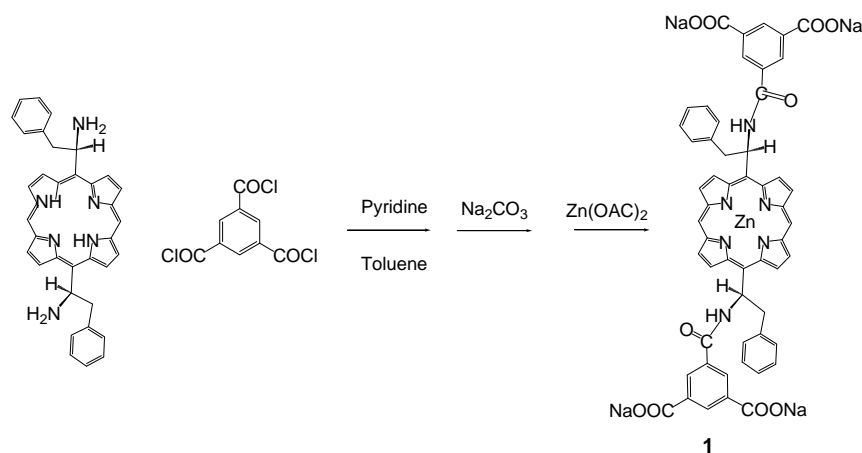
Porphyrin **4** (54.8 mg, 0.1 mmol) dissolved in 60 ml dry toluene was added dropwised very slowly to the solution of pyridine (2.0 ml) and benzene-1,3,5-tricarbonyl chloride (531 mg, 2.0 mmol in 60 mmol dry toluene). After the resultant mixture was heated up to 80°C and then stirred for 12 h, the mixture was cooled down and Na_2CO_3 aqueous solution was added to the reaction mixture slowly until the pH value of the aqueous layer is higher than 9. Then the mixture was heated up to 80°C and stirred until that the porphyrin was transferred into water layer. The water layer was

evaporated to dryness and methanol was added to the residue. After the mixture was filtered to remove most Na_2CO_3, the filtrate was concentrated to dryness, dissolved into water and with $Zn(OAc)_2$. Then the water solution was heated up to 80°C and then stirred for two hours. The mixture was cooled down, evaporated and subjected to column chromatography with H_2O/EtOH as the eluent to give purple solid **1.** Due to the poor solubility of **1** both in organic solvent (solubility in chloroform, methanol or THF is less than 0.05 mg/mL.) and water (solubility is *ca.* 0.5 mg/mL.), no ^{1}H NMR spectra suitable for analysis could be obtained both for (*R*)- and (*S*)-**1**. However, (*R*)- and (*S*)-**1** gave the same absorption and mass spectra. UV-VIS(CHCl$_3$): λ_{max}: 411, 553 and 583 nm. Maldi-TOF-MS (m/z) calcd for: C54H35N6Na4O10Zn: 1082.1. Found: 1082.3.

4. AFM image of the redissolved **1**:SWNTs
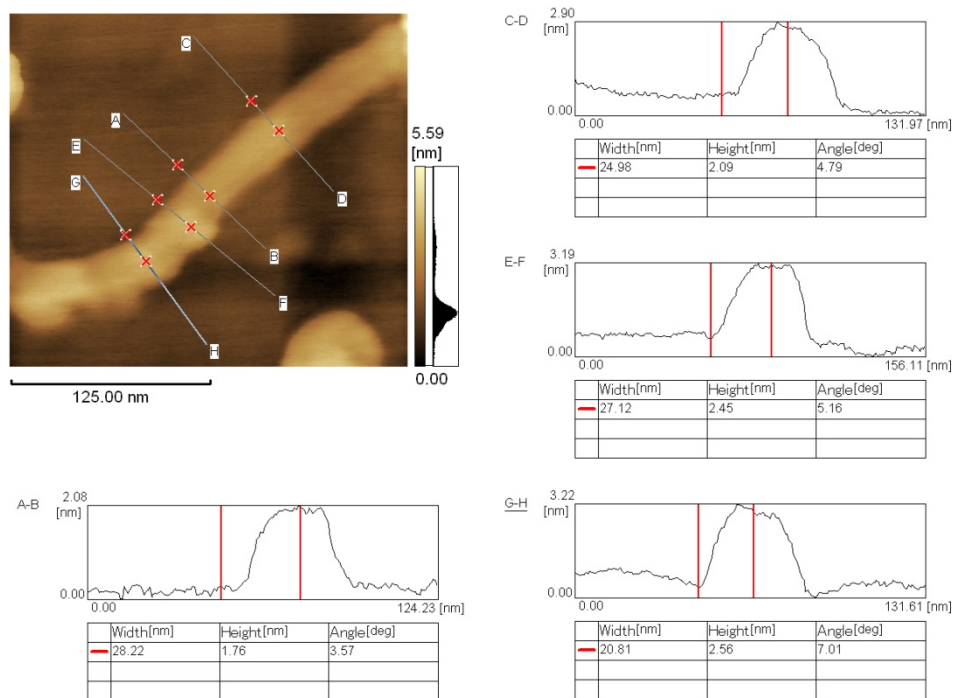
Figure S1. Height measurement of the tapping mode AFM image of the redissolved **1**:SWNTs kept more than 6 months.

20.65
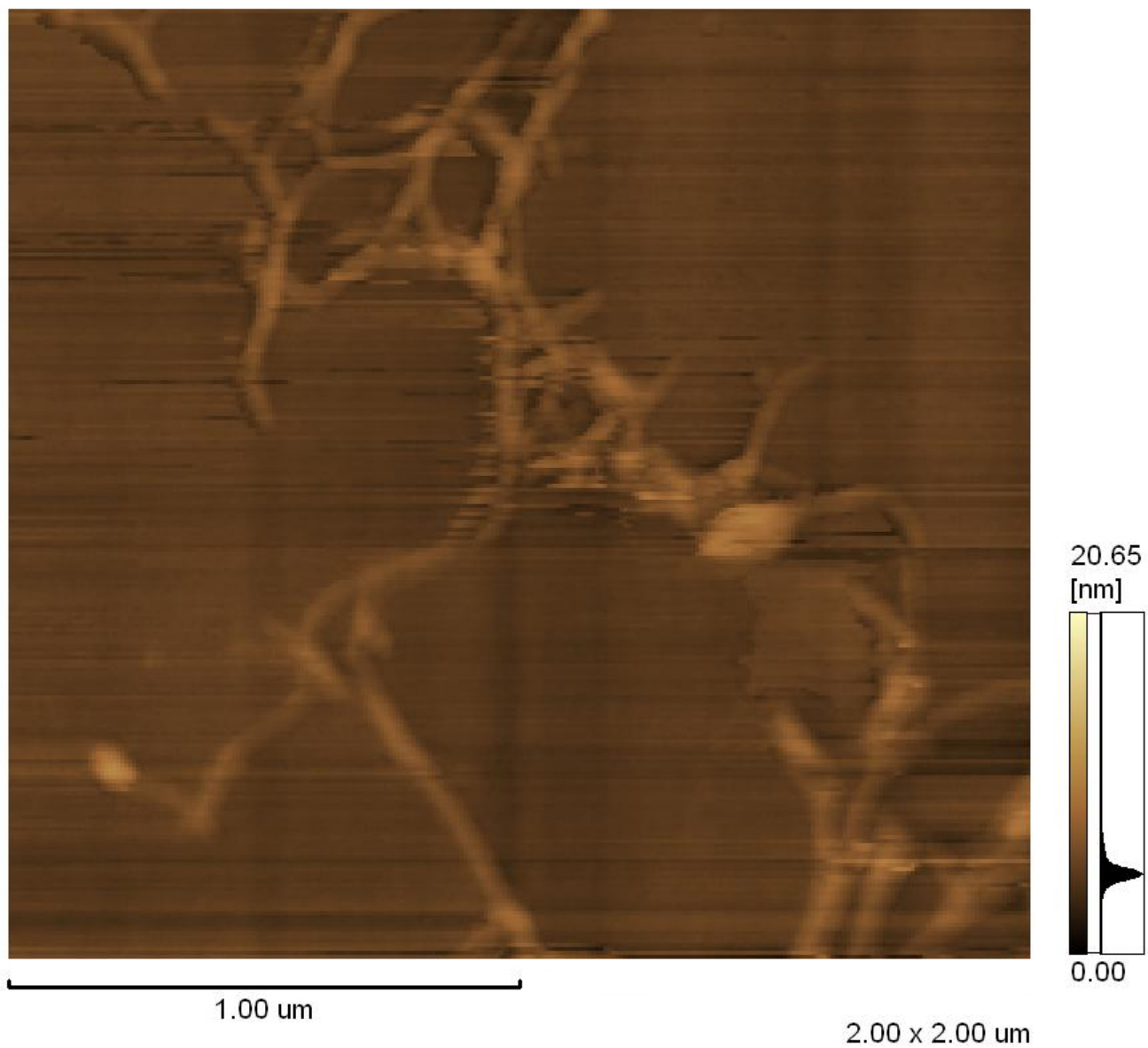[nm]

0.00

1.00 um

2.00 x 2.00 um

Figure S2. Tapping mode AFM image of the redissolved **1**:SWNTs kept more than 6 months.
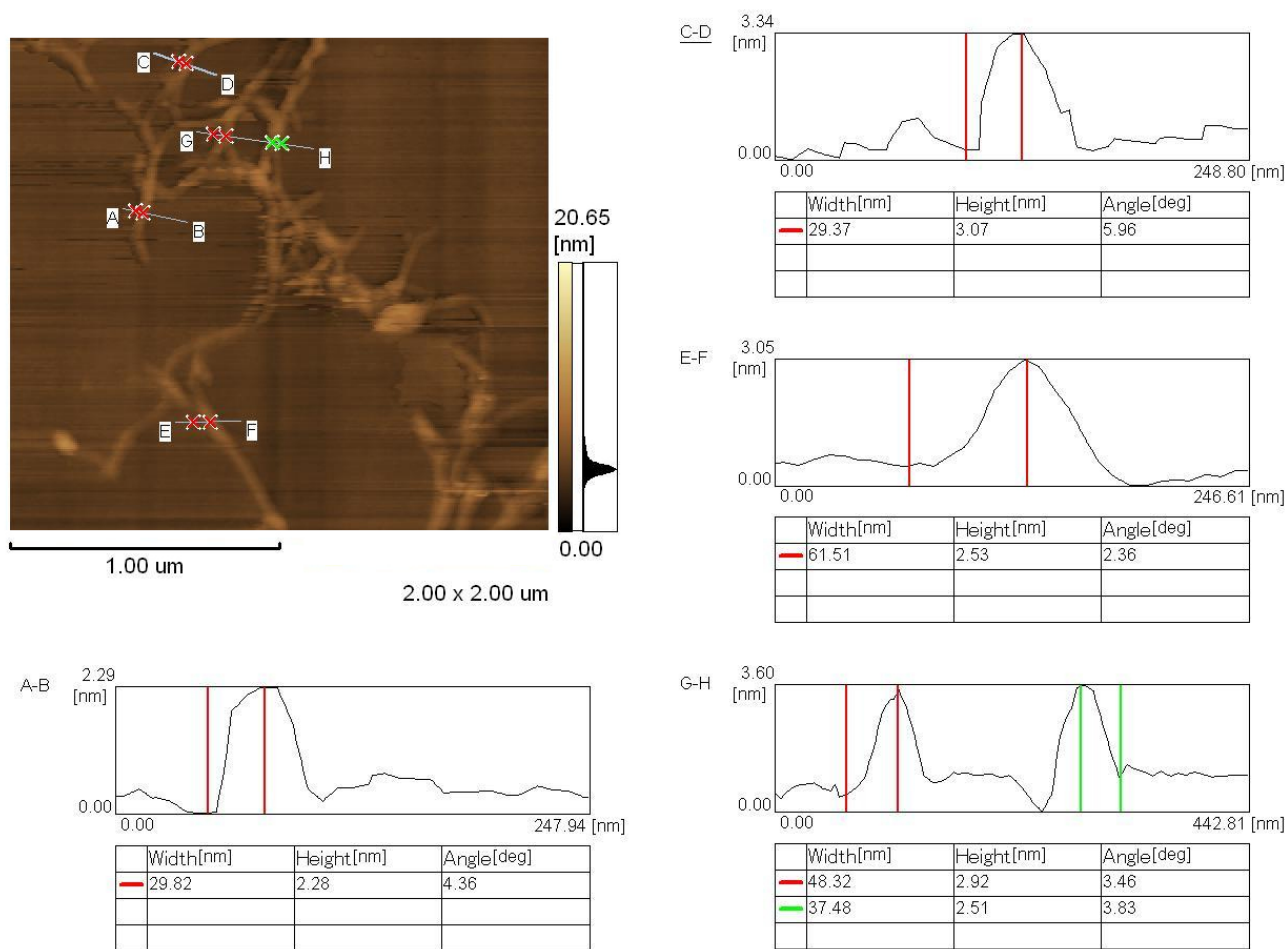
Figure S3. Height measurement of the tapping mode AFM image of the redissolved **1**:SWNTs kept more than 6 months.

5. Calculations of the conformational polymorphism of the chiral porphyrins on SWNTs

We used (6,5) SWNTs for the theoretical calculations because they are the main species in CoMoCAT, and the binding mechanism of the chiral porphyrins to (6,5)-SWNTs is estimated by molecular mechanics simulations. Energy-minimized calculations show that the porphyrin moiety and the two aryl groups fit very nicely along the curvature of the SWNT at distances of 3.56 and 3.59 Å (Figure 5), respectively, validating the presence of van der Waals interaction of the porphyrin moiety and the two phenyl groups with SWNTs. Computer generated (B)-(*R*)-**1**:(*M*)-(6,5)-SWNTs and (Z)-(*R*)-**1**:(*M*)-(6,5)-SWNTs (*M*, B and Z represent the left-handed helical alignment of SWNTs,[10b] the right- and left-handed wrapping of a chiral porphyrin, respectively.) two porphyrin conformations for the complexes of (*R*)-**1** with (*M*)-(6,5)-SWNTs, which is different from the calculations of chiral porphyrin/SWNTs complexes reported

previously.[10d] In the latter case, theoretical calculations generated only left-handed wrapping mode for the complex of (*R*)-**2** and SWNTs, and only right-handed wrapping mode for the complex of (*S*)-**2** and SWNTs. Because as-prepared chiral SWNTs are racemic thus consisted of (*M*)- and (*P*)-(6,5)-SWNTs (*P* represents the right-handed helical alignment of SWNTs.), calculations generated four different complex structures for (*R*)-**1** and (6,5) SWNTs, namely (B)-(*R*)-**1**:(*M*)-(6,5)-SWNTs, (Z)-(*R*)-**1**:(*M*)-(6,5)-SWNTs, (B)-(*R*)-**1**:(*P*)-(6,5)-SWNTs and (Z)-(*R*)-**1**:(*P*)-(6,5)-SWNTs. Similar to (*R*)-**1**, (*S*)-**1** also forms four different complex structures with (6,5)-SWNTs, as shown in Figure 5. Calculations also showed that the right-handed wrapping structures of (*R*)-**1** in (B)-(*R*)-**1**:(*M*)-(6,5)-SWNTs and (B)-(*R*)-**1**:(*P*)-(6,5)-SWNTs are more stable than the left-handed wrapping structures in (Z)-(*R*)-**1**:(*M*)-(6,5)-SWNTs and (Z)-(*R*)-**1**:(*P*)-(6,5)-SWNTs. On the other hand, the left-handed wrapping structures of (Z)-(*S*)-**1**:(*P*)-(6,5)-SWNTs and (Z)-(*S*)-**1**:(*M*)-(6,5)-SWNTs have more energy gain than the right-handed wrapping structures of (B)-(*S*)-**1**:(*P*)-(6,5)-SWNTs and (B)-(*S*)-**1**:(*M*)-(6,5)-SWNTs.
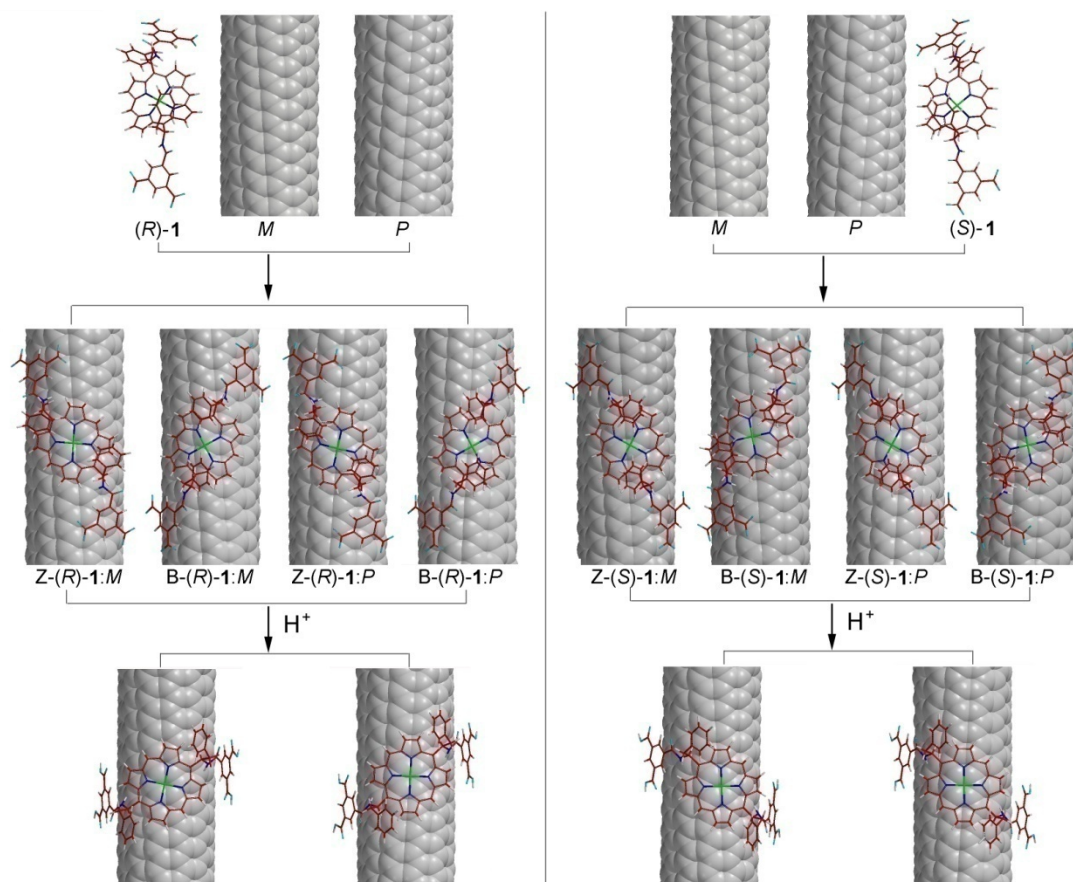

Figure S4. Computer-generated molecular modeling of the right- and left-handed wrapping of (*R*)- or (*S*)-1 with (*M*)- and (*P*)-(6,5)-SWNTs (please note that –COO⁻ were changed to –COOH after H⁺ were added.).